Contract No. F61775-00-WE027
Scientific and Technical Final Report

This material is based upon work supported by the European Office of Aerospace Research and Development, Air Force Office of Scientific Research, Air Force Research Laboratory, under Contract No. F61775-00-WE027. Any opinions, findings and conclusions or recommendations expressed in this material are those of the author(s) and do not necessarily reflect the views of the European Office of Aerospace Research and Development, Air Force Office of Scientific Research, Air Force Research Laboratory.

AN INVESTIGATION OF THE MOTION OF SPRING SUSPENDED PISTONS

Gordon Davey, Mike Dadd and Paul Bailey
Oxford University, Department of Engineering Science

INTRODUCTION

Linear compressors using flexure bearings and clearance seals have become an established technology in a number of applications, especially for Stirling and Pulse Tube cryocoolers. The advantage that they have over conventional compressors that use rotary drives is the combination of oil free operation, high reliability and long life.

A typical arrangement is shown in Figure 1. A piston and drive coil form a moving assembly that is suspended on a flexure bearing. The flexure bearings define a linear movement that is accurate enough to maintain a very small clearance between the piston and cylinder. Contacting or wearing surfaces that would require lubrication are eliminated and if the clearance is made small enough, seal leakage can be acceptable.

For good efficiency it is found that seal clearances need to be around 10 microns or less. To achieve this sort of clearance without contact requires accurate piston/cylinder components and also a bearing system that can provide an accurate linear movement. Flexure bearings, especially spiral disk have been found particularly good for such systems.

The cryogenics group at Oxford have built a number of cryocoolers of various designs and sizes. Satisfactory clearance seals have been achieved in all of these. Despite this it has been apparent for some time that our knowledge of the behaviour of flexure bearing systems has not been adequate. It is clear that the linearity of the movement is determined by accuracy of mounting surfaces and the alignment during assembly but the relative importance of various factors had not been established. We have generally assumed that the inner clamping surfaces and the alignment during assembly were crucial and designed components and assembly fixtures accordingly. However, we have not had any means by which we could directly relate the level of accuracy achieved with the resulting linearity.

REPORT DOCUMENTATION PAGE

Form Approved OMB No. 0704-0188

1. REPORT DATE *(DD-MM-YYYY)*	2. REPORT TYPE	3. DATES COVERED *(From – To)*
18-10-2002	Final Report	19 May 2000 - 19-May-01

4. TITLE AND SUBTITLE

AN INVESTIGATION OF THE MOTION OF SPRING SUSPENDED PISTONS

5a. CONTRACT NUMBER
F61775-00-WE027

5b. GRANT NUMBER

5c. PROGRAM ELEMENT NUMBER

6. AUTHOR(S)

Dr. Gordon Davey

5d. PROJECT NUMBER

5d. TASK NUMBER

5e. WORK UNIT NUMBER

7. PERFORMING ORGANIZATION NAME(S) AND ADDRESS(ES)
University of Oxford
Parks Road
Oxford OX1 3PJ
United Kingdom

8. PERFORMING ORGANIZATION REPORT NUMBER

N/A

9. SPONSORING/MONITORING AGENCY NAME(S) AND ADDRESS(ES)

EOARD
PSC 802 BOX 14
FPO 09499-0014

10. SPONSOR/MONITOR'S ACRONYM(S)

11. SPONSOR/MONITOR'S REPORT NUMBER(S)
SPC 00-4027

12. DISTRIBUTION/AVAILABILITY STATEMENT

Approved for public release; distribution is unlimited.

13. SUPPLEMENTARY NOTES

14. ABSTRACT

This report describes the investigation of the modeling and construction of low vibration mechanical compressors, such as used in cryogenic coolers. The classic 'Oxford' cryocooler has a clearance seal between the piston and the cylinder which is maintained by the use of spiral disc springs. In a typical compressor this clearance is about 12 microns, and therefore the spring suspension system must have a linearity of no more than 3 or 4 microns to avoid contact. It has always been assumed that to maintain this linearity, the surfaces between which the springs are clamped must be very flat and very parallel to each other. It has also been assumed that the flatness and parallel-ness of the clamping at the inside of the spring is more important than at the outside.

We investigate how the linearity of motion is dependent on the clamping conditions of the springs. Tests were carried out on a typical suspension system which was deliberately assembled between non-parallel clamping surfaces, and the linearity of the resulting motion was measured. A simple theoretical model was developed which gives good agreement with the experimental results.

15. SUBJECT TERMS
EOARD, Sensor Technology, Space Technology

16. SECURITY CLASSIFICATION OF:			17. LIMITATION OF ABSTRACT	18, NUMBER OF PAGES	19a. NAME OF RESPONSIBLE PERSON
a. REPORT	b. ABSTRACT	c. THIS PAGE			Ingrid Wysong
UNCLAS	UNCLAS	UNCLAS	UL	35	19b. TELEPHONE NUMBER *(Include area code)* +44 (0)20 7514 4285

The purpose of the work described here is to investigate how the linearity of movement is determined by the accuracy of components and their alignment. Ideally we would like to be able to estimate what tolerances need to be applied to the components and associated fixturing in order to achieve a specified linearity.

The aspects that need to be considered in order to achieve accurate linear movement of the flexure bearings can be broadly divided into the following areas:

- Geometrical accuracy of flexure bearing components:
  - Flexures – spiral springs in Oxford designs
  - Surfaces on which flexures are mounted.
- Alignment of flexure bearings during assembly.
- Mechanical properties of flexure bearing components.

The work described in this report concentrates on looking at the quality of the mounting surfaces and the alignment achieved during assembly. The flexures themselves are photo-etched to a high precision. They have always proved to be satisfactory providing care is taken in selecting material that has uniform thickness, acceptable flatness, and consistent mechanical properties.

The approach that has been taken is to build a test rig in which linearity measurements could be made on a well-defined bearing system – i.e. a system where the component and alignment accuracies could be measured. As far as was possible, these measurements looked at the effect of introducing a single geometrical deviation at a time. This was done to help achieve a clear relationship between cause and effect. A model of a flexure bearing system was also developed to form some framework for explaining the results.

The remainder of this report is structured as follows:

- Description Of Flexure Bearing Used
- Assembly of Flexure Bearing
- Measurement of Flexure Bearing Radial Movement
- Cases Investigated
- Measurement of Flexure Bearing Rotation
- Definition Of Component Geometry And Assembly Alignment
- Description Of Model
- Results from Model
- Comparison Between Model And Measured Values
- Conclusions

DESCRIPTION OF FLEXURE BEARING USED

A flexure can be defined as a component that allows movement by flexing i.e. changing shape. This is in contrast to most engineering bearings whose shape does not change and where movement is only possible between separate components. The attraction of flexures is that they can be used in combination to constrain motion without requiring sliding surfaces that are subject to wear.

The cryogenics group at Oxford has used flexures based on a flat spiral spring design as shown in Figure 2. In this geometry the flexing movement is produced by arms that connect inner and outer annuli. Flexing allows the planes defined by these annuli to move easily with respect to each other by rotation perpendicular to the flexure axis, displacement or a combination of both. When the inner and outer annuli are parallel, the displacement is along an axis perpendicular to the annuli. The movement that meets the greatest resistance in this type of flexure is a relative radial movement between the two annuli.

A flexure bearing is formed by spacing two sets of flexures apart and connecting the corresponding inner and outer annuli. If the flexures are mounted so that all the inner and outer annuli are parallel then it will be seen that a single displacement axis is defined. Radial movement or rotation perpendicular to this axis is strongly resisted on account of the radial movement that it causes in one or both of the springs. In this way the assembly behaves like a sliding bearing in that movement is constrained to a particular direction. Figure 3 shows a simple arrangement for a flexure bearing and identifies the mounting surfaces that ideally ought to be parallel.

When the mounting faces of the inner or outer annuli (or both) are not parallel the direction of displacement is not readily defined. Similarly, if both of these components have the mounting surfaces parallel, but the two components are angularly misaligned, the motion is difficult to define. In addition to the angular alignments of the mounting surfaces there are additional degrees of freedom that define the radial offsets between the flexures and mounting surfaces. This is illustrated in Figure 4.

ASSEMBLY OF FLEXURE BEARING

A schematic of the Test Assembly is shown in Figure 5. Two spiral springs are mounted on opposite ends of inner and outer cylinders to form a flexure bearing. The radial movement of the flexure bearing could be determined by measuring the run-out of an accurate bore, machined to be part of the inner cylinder.

The complete bearing was assembled on a roundness-measuring instrument called a TalyRond. This has a precise spindle, an adjustable turntable and gauges for the accurate measurement of run-out. Using this instrument it was possible to accurately align and measure the mounting surfaces during assembly.

MEASUREMENT OF FLEXURE BEARING RADIAL MOVEMENT

The experimental aim was, for the various configurations, to measure the linearity of motion of the flexure bearing assembly as it was taken through the full operational stroke. In a cryocooler, the motion would be provided by a linear motor. A suitable motor was not available, and the manufacture of one was beyond the scope of this project. Instead the flexure bearing assembly was mounted on an Instron Tensile Testing machine, and this was used both to provide the

necessary motion, and act as a displacement transducer. The test assembly is shown schematically in Figure 6, and photographically in Figure 7.

In a normal compressor the outside of the flexure bearing is fixed, with the inside moving, but this was reversed in the Test Assembly, with the inside supported in place by a 'pusher' fixed to the Base of the Instron, while the outside of the flexures was moved up and down by the Instron 'Crosshead'.

To eliminate any backlash, a heavy brass mass was added to the inside of the springs, so that when unsupported, the springs would droop under gravity by over 4mm. Initially the axial force was transmitted from the 'pusher' to the 'Inner Spacer' by means of a precision ball resting in a recess on top of the 'pusher' (shown diagrammatically in Figure 6). It was found that this arrangement could transmit transverse forces and thus affect the radial motion of the system, so a small thrust ball bearing race was added under the single ball (see Figure 8). With this new arrangement it was found that a considerable sideways force exerted on the 'pusher' would result in only a small ($\approx 0.1\mu m$) radial movement as measured by the Mu-Checker probe. It was thus determined that only purely axial forces could be transmitted to the inner cylinder of the Test Assembly.

The Mu-Checker probe was attached to a bracket above the assembly and could be positioned at twelve different angular positions, and at four heights (See Figure 7 and Figure 9).

The radial movement as recorded by the Mu-checker, and the axial displacement taken from the Instron were input to a Laptop computer via a data logger, and the results were then viewed and analysed using an Excel spreadsheet. Some typical results are shown in Figure 10, which shows repeatability at the sub-micron level.

CASES INVESTIGATED.

A variety of Inner and Outer Cylinders were manufactured so that the effect of a mis-alignment on both the inner and outer clamp faces could be studied. Four Outer Cylinders were made with the two faces out of parallel by 0.2, 0.4 and 0.6 mm, together with a parallel set. Four Inner Cylinders were made with the two faces out of parallel by 0.1, 0.2 and 0.3 mm, together with a parallel set. These misalignments were deliberately made much larger than the values normally expected in a Cryocooler, so that the resulting run-outs could be more readily detected. It was originally intended that tests on these components would lead to an empirical correlation between the misalignment and the resulting motion. In practice, however, only the parallel, and the worst cylinder of each type were used (the 0.3 Inner and the 0.6 Outer).

In total, four cases were investigated to varying degrees:-

1). Inner and Outer parallel and aligned.
2). Inner 0.3 tapered; outer parallel; aligned
3). Inner parallel; outer 0.6 tapered: misaligned.
4). Inner parallel; outer 0.6 tapered; aligned.

Initially tests were carried out at two angular positions – 0 degrees (in line with any misalignment) and at 90 degrees to this (clockwise when viewed from above). They were also made at two heights in the bore – at approximately 10mm and 37 mm from the top of the bore.

1. INNER AND OUTER PARALLEL AND ALIGNED

The tests on this specimen were carried out first (see Figure 11). The repeatability and run-out was less than 2 μm, which is similar in magnitude to the variation expected due to the cylindricity and surface finish of the bore.

2. INNER 0.3 TAPERED, OUTER PARALLEL; ALIGNED

These were the second set of tests carried out (Figure 12). These tests clearly showed that the run-out was poor in the direction of misalignment, but very good at right angles to this. It was noted that the slopes of the '90 deg' traces are of opposite signs to each other, and this hinted that the motion was not linear, but instead followed some form of curve instead of the linear motion that had been expected.

3. INNER PARALLEL; OUTER 0.6 TAPERED MISALIGNED.

To investigate further the results obtained in Case 2, for the third set of tests it was decided to make a more complete investigation of the motion produced by the suspension system. This was done by measuring the run out at 30° angular intervals, and at four different axial positions in the cylinder. By doing this, a true picture of the motion would be obtained.

A total of 48 sets of data were taken. It was found that each set of data could be well represented by a cubic polynomial, and so all of data was reduced to this form (see Figure 13).

All of the original data had an arbitrary origin; the Mu-checker probe was adjusted manually for each set of readings so that the readings were within the range of the instrument. The effect of this arbitrary origin was removed by adjusting the polynomials so that they all passed through the origin at mid-stroke (i.e. the run-out was zero) (Figure 14).

At each angular position, the 'curve fitted' data was then tabulated for the range of the stroke (Figure 15), and at 0.5mm intervals. From this, the mean of the four Mu-checker readings was taken to find the mean radial translation of the cylinder. In addition, each of the four readings was plotted against the height in the bore at which these readings were taken, and the slope of this is then equal to the angle of the cylinder bore. This data was then plotted as a function of axial position, and this is shown in Figure 16.

This plot uniquely characterises the motion in a single plane. It can be seen that both the slope of the cylinder and the radial translation are very nearly linear functions of the stroke, and these can thus be defined as a *Rate of Translation* (microns of radial deflection per mm of stroke) and a *Change of Slope* (microns/mm per mm of stroke)

This analysis was repeated for all twelve sets of data taken at 30° angles around the bore of the cylinder, and the results are plotted in Figure 17. The readings 180° apart are approximately equal and opposite to each other, which is confirmation that the methodology is correct and that the bore has good cylindricity. Interestingly, maxima are not aligned with the maximum taper on the components (at 0°) but are 30° away from this point.

As before, the alignment of the surfaces was measured on the Talyrond, and a summary of these is shown in Figure 18. These tests were carried out with a random alignment - the taper being unequally split between the top and bottom of the assembly.

4. INNER PARALLEL; OUTER 0.6 TAPERED: ALIGNED.

The assembly used in (3) above was assembled randomly, and the taper on the outer component was not distributed evenly between the top and the bottom. For case 4, the same components were then re-assembled making sure that the run-out of the Outer Cylinder, when measured, was equally distributed between the top and bottom surfaces of the cylinder. By doing this, the axes of the Inner and Outer Mounting surfaces were made co-linear, and hence there is minimum angular misalignment between the Inner and Outer Cylinders. A diagrammatic representation of this is shown in Figure 19.

When tested on the Instron machine, it was evident that the run-out for this assembly had been considerably reduced compared with case 3 above (Figure 20).

MEASUREMENT OF FLEXURE BEARING ROTATION

A characteristic of the flexure bearings is that provided all of the springs are stacked the same way round, there is a small rotation about the primary axis as the springs flex. This phenomena can be explained with reference to Figure 2; the spring arms are of constant length, so as the centre of the spring moves 'into the paper', the centre of the spring will have a small clockwise rotation. In a normal cryocooler, such a rotation is perfectly acceptable.

This rotation of the spring was measured so that it could be compared with the values calculated by the model. The match between the model and measured values would give some indication of the model's validity. The measurement was made by attaching an arm to the inner moving assembly and then measuring the tangential movement of the arm for varying axial positions. The results are shown together with model values in Figure 21.

DEFINITION OF COMPONENT GEOMETRY AND ASSEMBLY ALIGNMENT

In describing the geometry and alignment of a flexure bearing it is necessary to define a co-ordinate system. When the component geometry and alignment are perfect, the choice is fairly obvious – all the components are coaxial and perpendicular to a single axis that we could denote as the Z-axis. However, this is no longer the case if we allow imperfections in the mounting components and their alignment. In order to arrive at a convenient coordinate system the approach adopted is to generate the mounting surfaces from a single "mean" surface defined by equal and opposite displacements and rotations from the actual surfaces. This is described below with reference to Figure 22.

Consider a single annulus Ans0 in a section through its centre. It defines both a plane and an axis that is perpendicular to the plane and concentric to the annulus. The axis can be defined as the Z-axis and the plane of the annulus can be defined as the XY plane.

Annulus Ans0 can be rotated by an angle Ay each way about the Y-axis to generate two more annuli Ans1 and Ans2 as is shown. Ans1 and Ans2 can be rotated in a similar way about the X-axis through an angle Ax to generate two more annuli Ans3 and Ans4 (not shown). Finally these can be displaced in equal and opposite directions both along and perpendicular to the Z-axis to generate two further annuli Ans5 and Ans6.

It will be seen that by starting with a single annulus, two misaligned and separated annuli have been created that correspond directly to one set of mounting surfaces of a flexure bearing. It follows from this that the misalignments present in a flexure bearing can be completely defined in the following way:

<u>Outer mounting surfaces</u>:
Coordinates X, Y, Z
Angular misalignments about X and Y axes: Aox and Aoy
Radial Offset along X and Y axes: Rox and Roy
Separation between mounting surface along Z axis Doz

<u>Inner mounting surfaces</u>:
Coordinates X^i, Y^i, Z^i
Angular misalignments about X and Y axes: Aix and Aiy
Radial Offset along X and Y axes: Rix and Riy
Separation between mounting surface along Z axis Diz

<u>Alignment during assembly</u>
With the above descriptions of inner and outer mounting surfaces, alignment during assembly can be defined in terms of the relationship between the two coordinate systems (X, Y, Z) and (X^i, Y^i, Z^i). It follows from this that in the most general case six parameters need to be specified. Three angles are used to define a rotation of interim axes with respect to X, Y, Z as shown in Figure 23. An axis is defined by means of two angles B1and B2. A third angle B3 then defines a rotation about this axis. (Figure 23 actually shows the general three-dimensional rotation of a point about fixed axes but it can be seen that this is equivalent to fixing the point and rotating the

axes). The remaining three parameters Mx, My and Mz then define the translation of the transformed axis along the X, Y, and Z axes.

Transforming Coordinates Between Coordinate Systems

The equations used to transform coordinates in the $X^iY^iZ^i$ coordinate system to the XYZ coordinate system are given in Appendix 1.

DESCRIPTION OF MODEL

Modelling the movement of the flexures using finite element methods was considered to be beyond the scope of this work and instead a very much simpler approach was adopted. This approach is described below for the spiral spring type of flexure used at Oxford.

If a single spiral spring arm is considered in isolation it is found that its stiffness is very different in different directions. Referring to Figure 24 the direction of least stiffness is for relative movement between Pi and Po along the Z-axis (i.e. out of the paper). This is because the movement constitutes the bending of a thin section – the minimum spring arm width being typically 5 to 10 times the spring thickness. This direction corresponds to the direction of movement in a flexure bearing.

The direction with the next lowest stiffness is along the Y-axis, again a bending movement perpendicular to the arm, but this time in the plane of the flexure. The stiffness is higher because the section is thicker and the stiffness varies according to the cube of the thickness.

Finally the direction in which the stiffness is highest is along the arm. This movement corresponds to tension and compression of the arm without any bending. For spring arms that do not have high angles of curvature, this can be approximated by defining the direction as the line joining the two ends of the arm i.e. line Pi to Po along the X-axis in Figure 24.

From these considerations, the idea emerges that stiffness along the Y and Z axes can be ignored and that the movement of the spring arms will be determined solely by considering the strain along the arm i.e. in this approximation, the X axis. Each spring can then be treated as an assembly of struts. The struts can pivot at their attachment points, they can extend or contract but they are assumed not to bend.

This approach is clearly a fairly gross simplification and would not be satisfactory if the model was intended to give accurate values of the spring movement. For the purposes of this study however it was thought that the general behaviour and magnitudes that it generated might be close enough to be useful.

The more detailed assumptions for the model are:

- A four-arm spring is modelled for simplicity. It is assumed that characteristics demonstrated will be applicable to the six arm springs that are more frequently used.

- To a first approximation the motion of the flexure bearing will be the motion that causes least strain along the flexure arms.

- The arms are modelled as extendable struts mounted between inner and outer components.

- The struts are mounted such that they can freely pivot about their mounting points.

- The struts are assumed not to bend.

- If the spiral springs are prevented from rotating then the strain in opposite sets of arms is assumed to be equal.

- If the springs are allowed to rotate then for typical spring designs a movement can be defined which results in zero extension along the arms.

A complete flexure bearing is modelled as shown in Figure 25. There are two single springs each represented by four struts. The struts are attached at their ends (at points P_{xo1} and P_{xi1} etc) to inner and outer hollow cylinders, the mounting surfaces being the annuli defined at each cylinder end. Points P_{xo1} and P_{xi1} etc are defined as the points at the ends of the arms as shown in Figure 24. The spring clearly does not pivot in such a well-defined way but this definition is regarded as adequate for this model.

The geometry of the mounting surfaces in the model is defined as described in a previous section. The attachment points, P_{xo1} etc, on the outer cylinder are described in terms of a XYZ coordinate system. The attachment points, P_{xi1} etc, on the inner cylinder are similarly described in terms of a $X^iY^iZ^i$ coordinate system.

The assembly alignment is set by defining the angular and displacement transformations between the two coordinate systems, i.e. values for B1, B2, B3, Mx, My and Mz. For example, a perfect alignment of the mounting surfaces would be modelled by setting all the angles and offsets to zero except for B3, which is set to the appropriate spiral angle for the spring. For the spring investigated the angle B3 between points P_{xo1} and P_{xi1} was around 90 degrees.

With the geometry of mounting surfaces defined and the assembly alignment set the flexure movement is determined as follows.

1. The initial coordinates of the points P_{xi1}, P_{xo1} etc are calculated for all the struts.

2. The coordinates are used to calculate the initial lengths of all the struts. These lengths represent the unstressed condition of the struts as they are initially assembled.

3. The flexure bearing movement is modelled by changing the Z offset Mz between the coordinate systems i.e. the origin of the $X^iY^iZ^i$ coordinate system is displaced a given amount along the Z axis. All the other alignment parameters are unchanged.

4. For this new state the coordinates are recalculated. This is only necessary for the points that have moved i.e. the points on the inner cylinder.

5. The lengths of the struts are recalculated using this new set of coordinates.

6. The differences between the new lengths and the original lengths are calculated. These values represent the amount of strain in each strut.

7. The alignment parameters B1, B2, Mx and My are then adjusted so that the strains in opposing struts are the same. This in effect balances the forces acting on the struts.

8. In addition the angle B3 can be adjusted such that one of the strut lengths returns to its initial unstressed length. Although this adjustment is only made on the basis of one strut, it is found that all the strut lengths return very closely to their original length.

By repeating steps 3 to 8 with different values of Mz over a chosen operating range, the movement of the flexure bearing can be investigated. In addition the actual run out that would be measured can be calculated for any piston or cylinder assembly attached to the flexure spring.

In the work described here the model was executed in an Excel spreadsheet using the solver facility. Model solutions were found by:

1. Calculating the differences between the strain in opposing struts and then requiring the solver to minimise the sum of the squares of these values by adjusting B1, B2, Mx and My.

2. Requiring the solver to minimise the difference between the length of one strut and its original length by adjusting B3

RESULTS FROM MODEL

There are a large number of possible combinations of misalignments that could be investigated with this model. However, for the purpose of understanding the effect of particular misalignments cases considered were kept as simple as possible and were as follows:

- Perfect mounting surfaces and perfect assembly alignment – this was done to check that the model did not give an obviously wrong answer. Equivalent to experimental Case 1.

- Case #5 Inner mounting surfaces not parallel, all other surfaces and alignments being perfect. This is equivalent to experimental Case 2.

- Case #6 Outer mounting surfaces not parallel, all other surfaces and alignments being perfect. Equivalent to experimental Case 4.

- Case #7 Assembly with angular misalignment between axes, inner and outer mounting surfaces being perfect.

- Case #8 Inner mounting surfaces not parallel and angular misalignment during assembly, Outer mounting surfaces perfect.

- Case #9 Radial offset of one inner mounting surface with respect to the other, all other surfaces and alignments being perfect.

With the all the mounting surfaces parallel and perfect alignment during assembly it was confirmed that the model predicts minimal run-out – the residual values generated were attributable to the accuracy set in the solver.

The movement of the bearing can be expressed as the variation of B1, B2, B3, Mx and My, with axial position but these values are not immediately helpful. The results can be more usefully displayed by showing the run out that would be measured in the XZ and YZ planes. This is done for the remaining cases shown in Figure 26 to Figure 40.

Figure 26 to Figure 28 show the run-outs for Case #5 where the inner mounting surfaces have a taper between them of 0.3 mm over a distance of 55 mm. This corresponds to angle Aix = 0.156 deg.

Figure 29 to Figure 31 show the run-outs for Case #6 where the outer mounting surfaces have a taper between them of 0.6 mm over a distance of 130 mm. This corresponds to angle Aox = 0.132 deg.

Figure 32 to Figure 34 show the run-outs for Case #7 where the inner and outer mounting surfaces are parallel but the there is an angular misalignment on assembly of 0.1 deg i.e. B1 = 0.1 and let B2 = 0.

Figure 35 to Figure 37 show the run-outs for Case #8 where there is a combination of a taper of 0.3 mm between the inner mounting surfaces and an assembly misalignment of 0.1 deg, This corresponds to angle Aix = 0.156 deg with B1 = 0.1 and B2 = 0.

Figure 38 to Figure 40 show the run-outs for Case #9 where there is a radial offset of 0.2 mm between top and bottom inner clamping surfaces.

The model results show that the flexure bearing movement is affected in different ways depending on the nature of the misalignment.

In Cases #5 and #6 where the inner and outer mounting surfaces are not parallel but assembly alignment is perfect, the behaviour is similar and the main features are:

- The run-out depends very much on the axial position of the measurement. At the centre of the flexure bearing the run-out is small. The run out increases linearly with the distance from the centre and becomes significant for quite small distances. This effect is

particularly important if sealing surfaces are cantilevered out from the flexure spring assembly.

- The run-out is not a linear function of spring movement. The movement varies with the axial position of the measurement. However the run-out is symmetric about bearings centre.

- For measurements at axial positions away from the centre the run-out changes monotonically as the bearing moves from one end of its range to the other. In contrast the run-out measured near the centre reverses as the bearing moves through its midpoint.

- Although the tapers between the surfaces are along the X-axis, the run-outs measured show components in both the X and Y directions.

In Case #7 where the mounting surfaces are parallel but the assembly has an angular misalignment, the behaviour is very different and the main features are:

- The run-out is independent of the axial position of the measurement.

- The run-out is a linear function of spring movement.

- Although the assembly misalignment was about the Y-axis, the run-outs measured show components in both the X and Y directions.

- The angular misalignment was set in the ZY plane (i.e. about the X-axis) and the run out is also mainly in the YZ plane. The run-out in the XZ plane is approximately one sixth of the YZ value.

Case #8 is a combination of cases #5 and #7 and shows how the two effects can combine. It is noted that this is not a unique combination as the angular orientation between the two effects is an independent variable. As a consequence, combinations can result in more or less run out than the individual components.

In Case #9 where there is a 0.2 mm offset between the top and bottom inner mounting surfaces the main features are:

- The run out is relatively small in both directions.

- The run out is not a linear function of spring movement. In particular the run-out is not symmetric about the centre.

For all the cases it was found that for any axial position an angle could be found in the XY plane where the measured run-out would be small.

The variation of B3 with axial position determines how the spring rotates as it moves. Figure 21 shows the rotation calculated by the model together with measured values. The absolute vales calculated by the model are significantly higher than the measured values however the functional variation is very similar. If the model values are multiplied by 0.62, then these adjusted values (the 'Ad Mod' values in Figure 21) are very close to the measured values.

COMPARISON BETWEEN MODEL AND MEASURED VALUES

Two of the experimental cases were analysed using the theoretical model, Case 2 being modelled in Case 5, and Case 4 modelled by Case 6:

> **Cases 2 and 5**. In Figure 12, the '0 degree' readings correspond to the model 'x' direction shown in Figure 26, and the '90 degree' readings correspond to the 'y' readings shown in Figure 27. The 'top' values are equivalent to 'z = +20', and the 'bottom values are equivalent to 'z = -10' in the model results. Comparison of the experimental and test results show similar qualitative behaviour, the most significant difference being that the run-out measured are about 4 times higher at '0 deg' than at '90 deg', whereas the model 'x' and 'y' directions differ by a factor of only 2.
>
> **Cases 4 and 6.** The experimental results given in Figure 20 correspond to the modelling shown in Figure 29. The 'top' values correspond to the 'z = +20', and the '2nd bottom' to 'z = -10'. The comparison between the two is good: both show the slope of the run-out changing from negative to positive as measurement position goes from top to bottom of the bore. The magnitudes also compare well - it must be remembered that the experimental results include an element due to the imperfect geometry of a real cylinder, whereas the model results assume a perfect cylinder.

CONCLUSIONS

Considerable difficulty was encountered in assembling, aligning and measuring the test pieces in a way that could be readily defined and compared with the theoretical model. However, there is evidence to show that the model does predict the motion that could be expected from a misaligned flexure bearing system. Were sufficient resources available, some of these tests could have been repeated, and it is likely that more agreement would be reached.

Though not verified experimentally, the modelling does show that different types of misalignment lead to different forms of run-out behaviour.

The following conclusions can be drawn from this work:

- Alignment can be described by angular and offset parameters that define deviations from perfect alignment.

- The angular alignment of a pair mounting surfaces (e.g. outer or inner) can be expressed as half angles relative to a mean plain.

- The alignment between inner and outer mounting surfaces that is achieved during assembly has a significant impact on the final run-out. This alignment can be defined by the angular disposition of the two mean planes with respect to each other.

- By studying the shape of the curve obtained from run-out measurements, some idea of the geometric cause of the run-out can be determined.

- If both inner and outer flexure mounting components are not parallel, it is unlikely that good linearity will be obtained.

- The maximum run-out measured may not occur at the same angular position of maximum taper on the flexure mounting surfaces.

- For typical assemblies, the model shows that angular misalignments are more significant than offset ones.

- Tapered mounting surfaces result in a curved motion, and a run-out that is very dependent on the axial position of measurement. The run-out measured half way between the flexures can be very small even for significant tapers. Measurements further out will give much greater values.

- If run-out measurements are used to verify the alignment of a flexure bearing, there should be at least two sets of measurements taken as far apart axially as is possible.

- Angular misalignment during assembly will give a run-out that is linear with flexure deflection and independent of axial position.

- The model appears to predict generally the right qualitative and quantitative behaviour. However it is not very accurate in predicting the right angular orientation of the run out.

Gordon Davey
Mike Dadd
Paul Bailey

29th July 2002

APPENDIX 1

TRANSFORMATIONS IN THREE DIMENSIONAL GEOMETRIES

GENERAL ROTATION IN 3D

Any combination of rotations in three dimensions can be generally represented by a single rotation about a particular axis.

Referring to Figure 23:

OM is an axis around which *P1* is to be rotated to give *P2*.
$\overline{N}$ is a unit Vector is a unit vector along *OM*

$\overline{N}$ is given by: $\overline{N} = l.\bar{i} + m.\bar{j} + n.\bar{k}$

l, m and *k* are determined from rotation angles *B1* and *B2* by

$$l = \sin(B1).\cos(B2) \qquad m = \sin(B1).\sin(B2) \qquad n = \cos(B1)$$

A plane normal to OM containing point P1 can be defined by

$$\overline{OP1}.\overline{N} = d \qquad\qquad d = l.x + m.y + n.z$$

OP1 is the vector from *O* to point *P1*

$$\overline{OP1} = x.\bar{i} + y.\bar{j} + z.\bar{k}$$

Q is the point at which *OM* intersects the plane and *d* is the distance *OQ*

$$\overline{OQ} = d.\overline{N}$$

$\overline{QP1}$ is a vector from Q to P1 that lies within the defined plane. A vector $\overline{QS}$ of equal length can be defined that is perpendicular to $\overline{QP1}$ which also lies in the defined plane.
Any rotation of P1 about the axis OM through an angle of B3 can then be represented by vector $\overline{QP2}$ where

$$\overline{QP2} = \cos(B3).\overline{QP1} + \sin(B3).\overline{QS}$$

$\overline{QS}$ can be found by forming the vector product $\overline{OP1} \times \overline{N}$

$$\overline{QS} = \overline{OP1} \times \overline{N} \qquad \overline{QS} = \begin{vmatrix} \bar{i} & \bar{j} & \bar{k} \\ x_1 & y_1 & z_1 \\ l & m & n \end{vmatrix} = (n.y_1 - m.z_1).\bar{i} + (l.z - n.x).\bar{j} + (m.x - l.y).\bar{k}$$

$$\left|\overline{QS}\right| = \sqrt{(n.y - mz)^2 + (l.z - n.x)^2 + (m.x - l.y)^2}$$

$$\overline{OP2} = \overline{OQ} + \overline{QP2} = \overline{OQ} + \cos(B3).\overline{QP1} + \sin(B3).\overline{QS}$$

$$\overline{OQ} = d.(l.\bar{i} + m.\bar{j} + n.\bar{k})$$

$$\overline{QP1} = (x - dl).\bar{i} + (y - dm).\bar{j} + (z - dn).\bar{k} \qquad \left|\overline{QP1}\right| = \sqrt{(x - dl)^2 + (y - dm)^2 + (z - dn)^2}$$

$$\overline{QS} = (n.y - m.z).\bar{i} + (l.z - n.x).\bar{j} + (m.x - l.y).\bar{k}$$

$$\overline{OP2} = \left[dl + \cos(B3).(x - dl) + \sin(B3).(n.y - m.z)\right]\bar{i} + \left[dm + \cos(B3).(y - dm) + \sin(B3).(l.z - n.x)\right].\bar{j} + \left[dn + \cos(B3).(z - dn) + \sin(B3).(m.x - l.y)\right]\bar{k}$$

Point P2 can be defined by transformed coordinates x', y', z' given by

$$x' = dl + \cos(B3).(x - dl) + \sin(B3).(n.y - m.z)$$

$$y' = dm + \cos(B3).(y - dm) + \sin(B3).(l.z - n.x)$$

$$z' = dn + \cos(B3).(z - dn) + \sin(B3).(m.x - l.y)$$

COMBINED ROTATION AND TRANSLATION

A translation can be combined with the rotation to give a new point P3 with coordinates x'', y'', z'' defined by:

$$x'' = x' + x_0 \qquad y'' = y' + y_0 \qquad z'' = z' + z_0$$

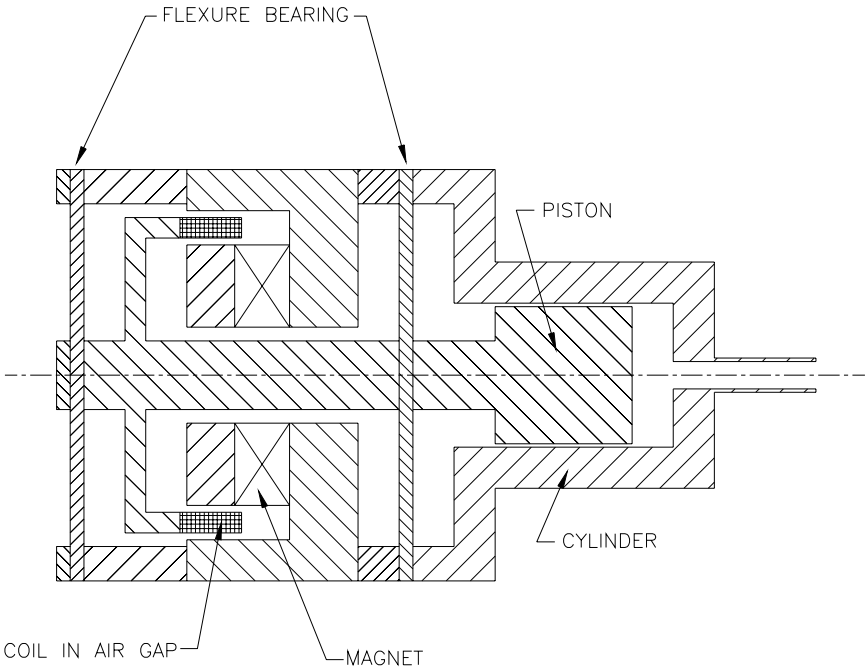

Figure 1. Typical Cryocooler Suspension System.

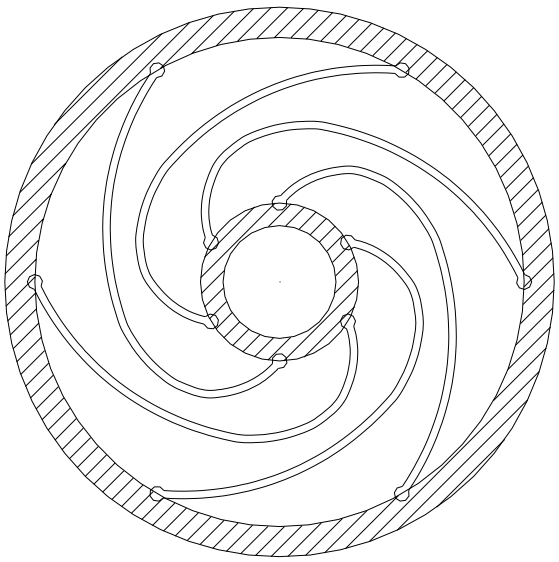

Figure 2. Typical Spiral Spring. The hatched areas are where the spring is clamped.

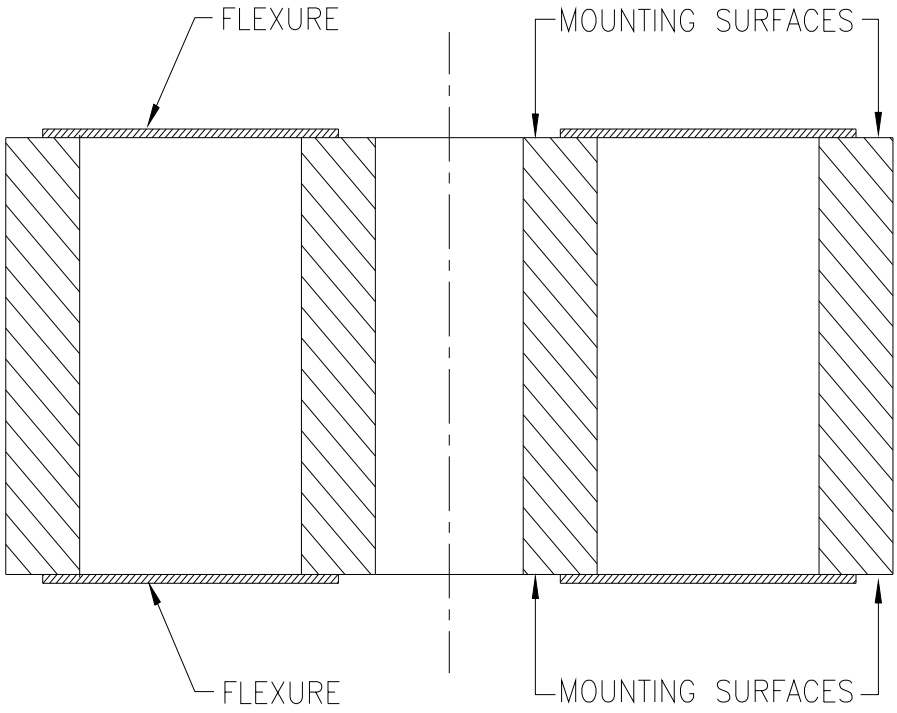

Figure 3. Section Through Simplified Flexure Bearing Assembly.

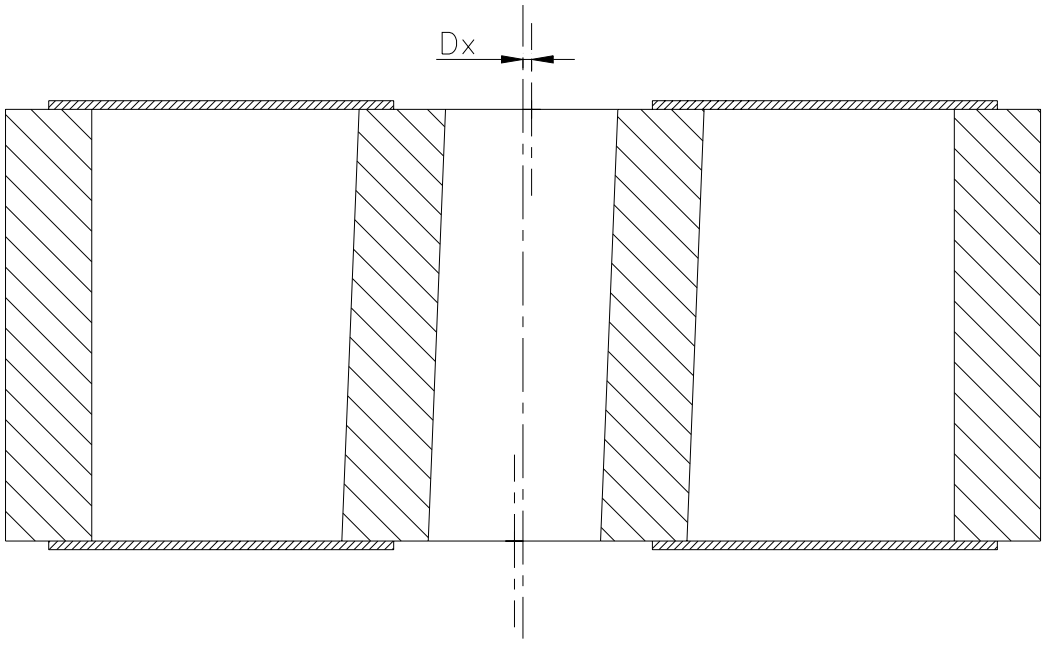

Figure 4. Radial Offset between Flexure and Mounting Surface.

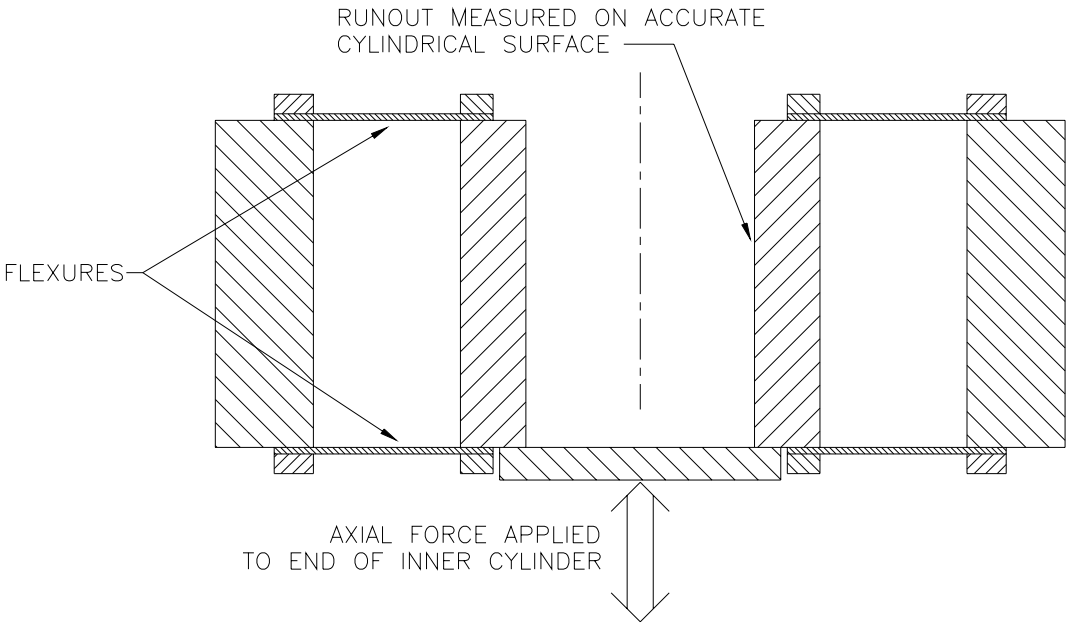

Figure 5. Test Assembly

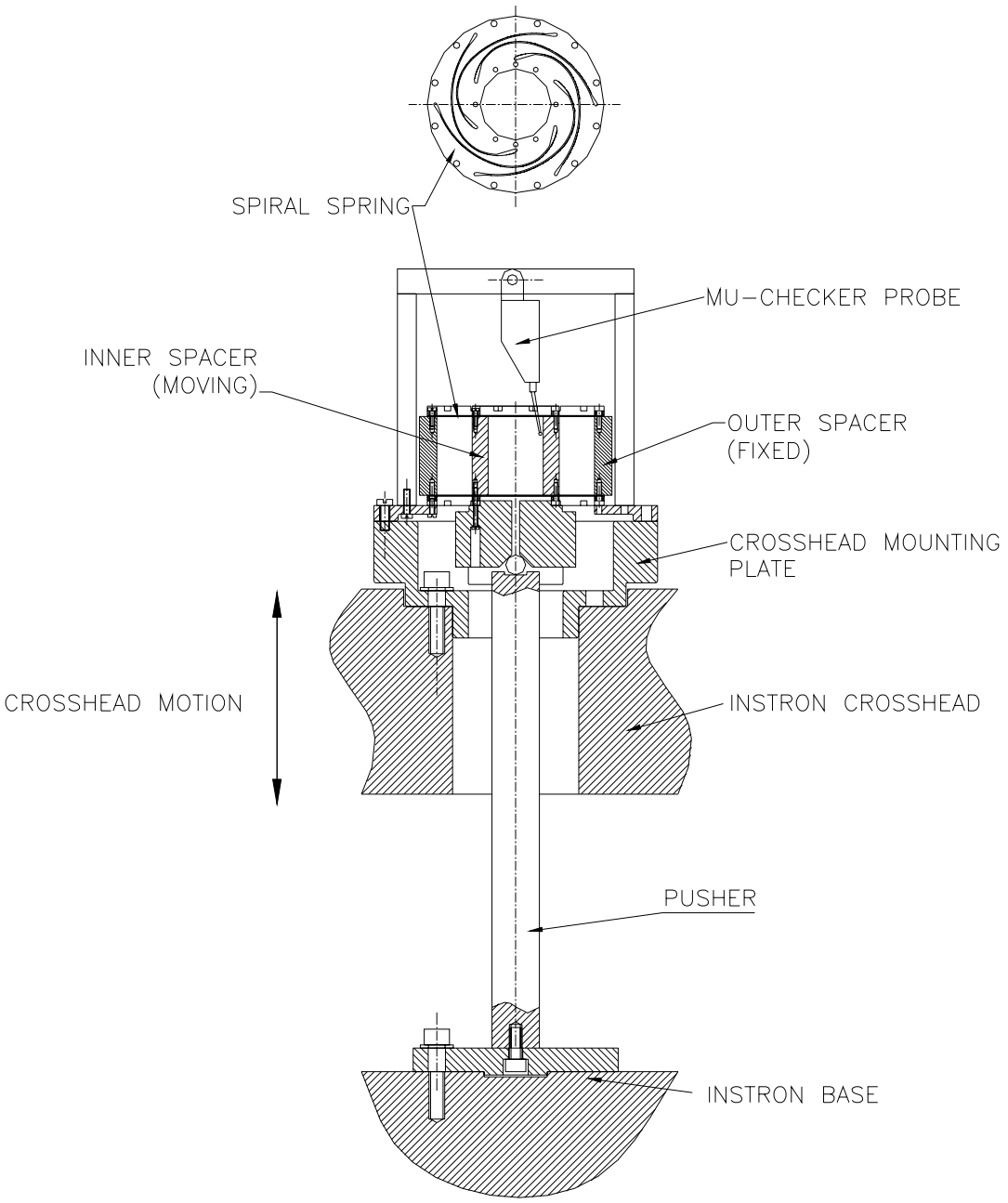

Figure 6. Instron Test Assembly for Measuring Run-out.

Figure 7. Instron Test Assembly. The flexures are hidden at the top, and above them the Mu-Checker probe for measuring the Run-out is visible.

Figure 8. Top of 'Pusher' of Test Assembly, showing a Thrust Ball Bearing Race underneath the single precision Ball Bearing.

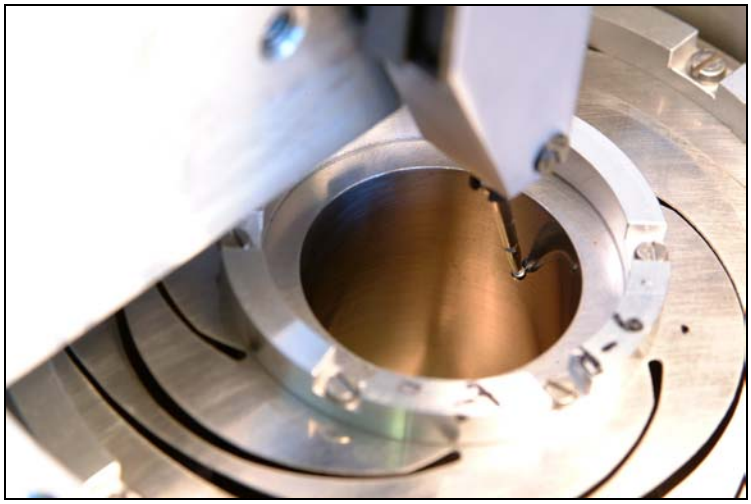

Figure 9. View of Mu-Checker Probe in Bore of the Test Assembly.

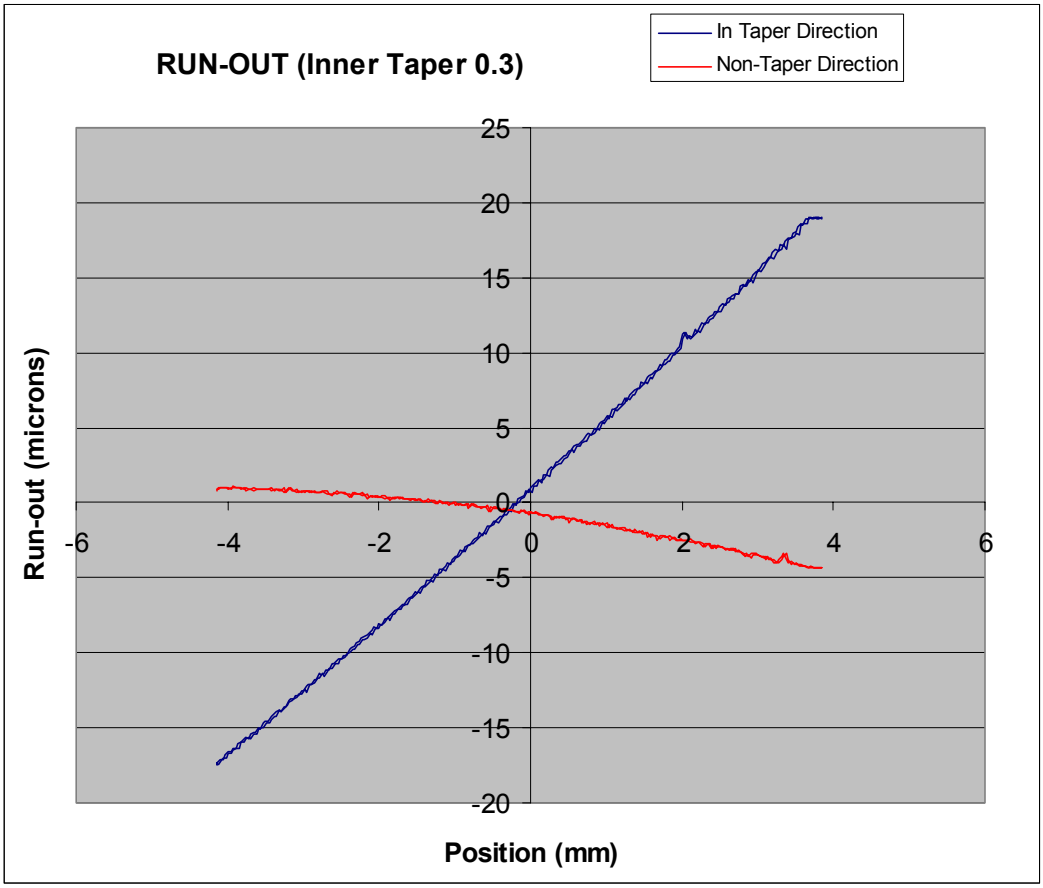

Figure 10. Typical Run-out Test Results. The run-out as measured by the Mu-Checker is plotted against axial position. The traces show repeatability at the sub-micron level.

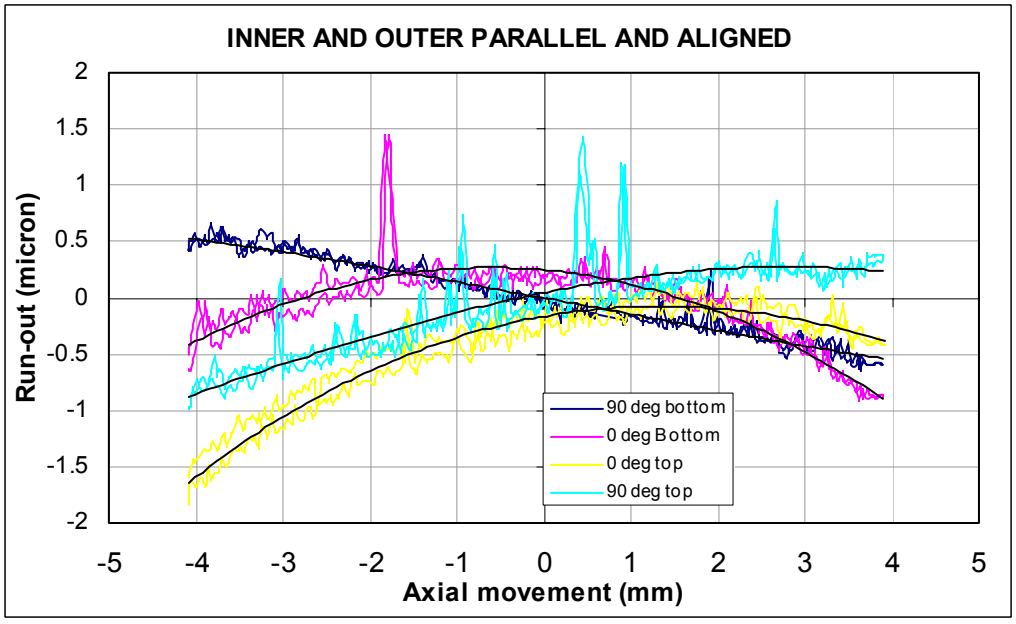

Figure 11. Inner and Outer Parallel. The run-outs detected here are not significantly higher than those expected from the cylindricity of the surface of the inner spacer.

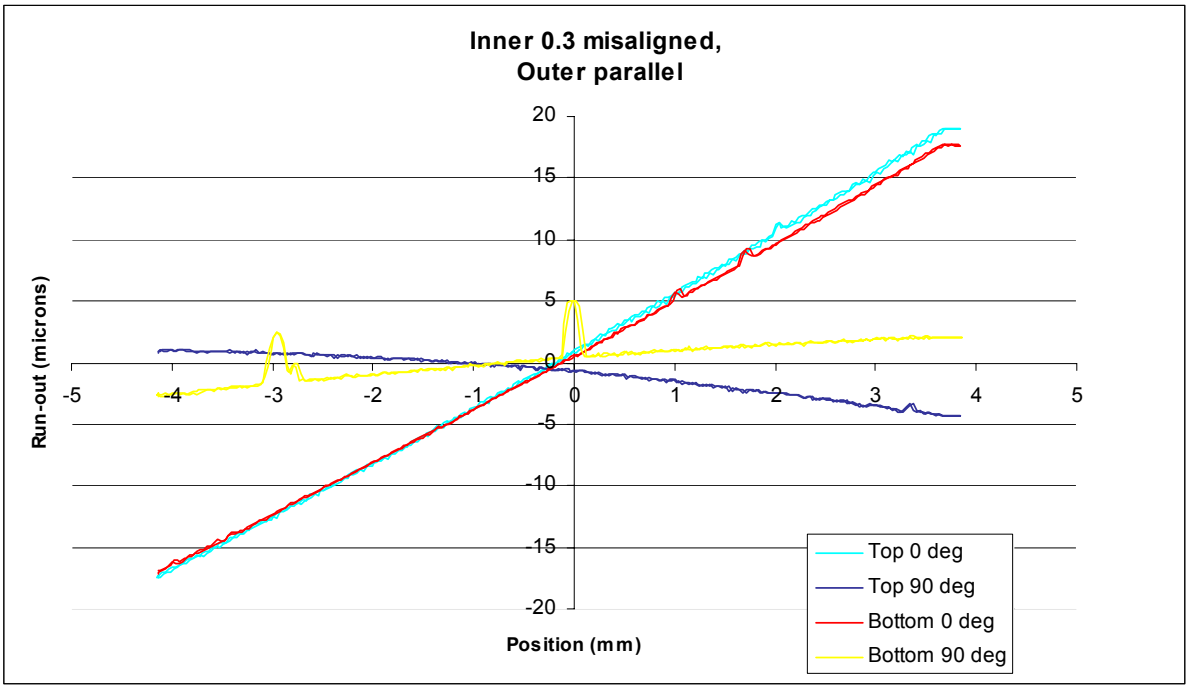

Figure 12. Case 2 results: Inner 0.3 Misaligned, Outer Parallel. The '0 deg' readings are in the direction of misalignment. Note that the slopes of the '90 deg' are of opposite signs.

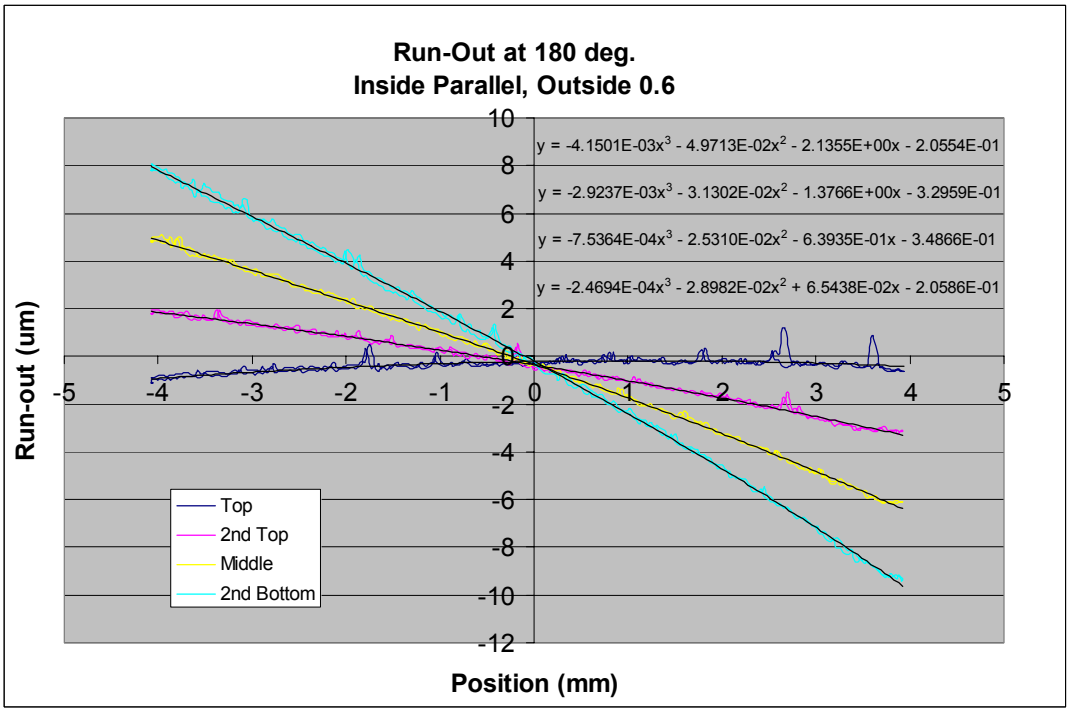

Figure 13. Case 3 Test Results. Note how the run-out is almost perfect at the top, but very bad at the bottom. The motion is clearly following a curve. Polynomial curve fitting describes the motion well.

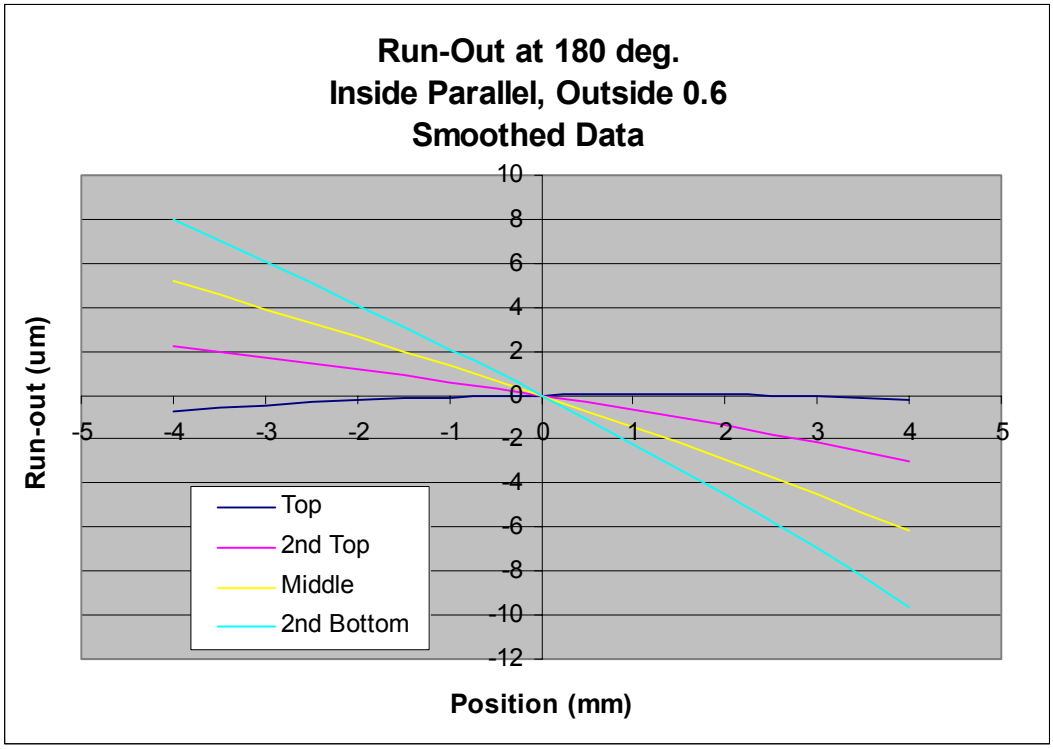

Figure 14. Case 3 Test Results – Polynomial Curve fit (adjusted to pass through the origin).

Distance from								
Top of Inner:-	9.85	18.85	27.85	36.85				
	TOP	2nd	Mid	4th				
Position	Run-out	Run-out	Run-out	Run-out		mean	Slope	Position
(mm)	(micron)	(micron)	(micron)	(micron)				(mm)
-4	-0.70965	2.20067	5.192724	8.012392		3.674033	0.32398	-4
-3.5	-0.57347	1.959987	4.560038	7.043371		3.247482	0.282784	-3.5
-3	-0.45048	1.710606	3.92705	6.071281		2.814614	0.242019	-3
-2.5	-0.34087	1.451961	3.291568	5.093011		2.373917	0.201569	-2.5
-2	-0.24483	1.183488	2.651399	4.105446		1.923877	0.161319	-2
-1.5	-0.16253	0.90462	2.004351	3.105476		1.462979	0.121153	-1.5
-1	-0.09417	0.614793	1.34823	2.089986		0.989709	0.080955	-1
-0.5	-0.03993	0.313441	0.680844	1.055865		0.502554	0.040609	-0.5
0	0	0	0	0		0	0	0
0.5	0.025443	-0.3261	-0.69649	-1.08072		-0.51947	-0.04099	0.5
1	0.036209	-0.66541	-1.41083	-2.18941		-1.05736	-0.08247	1
1.5	0.032114	-1.01852	-2.14521	-3.32919		-1.6152	-0.12456	1.5
2	0.012973	-1.38597	-2.90181	-4.50315		-2.19449	-0.16738	2
2.5	-0.0214	-1.76834	-3.68284	-5.71443		-2.79675	-0.21104	2.5
3	-0.07119	-2.16619	-4.49048	-6.96612		-3.42349	-0.25566	3
3.5	-0.13658	-2.58008	-5.32693	-8.26134		-4.07623	-0.30135	3.5
4	-0.21776	-3.01059	-6.19438	-9.60321		-4.75649	-0.34822	4

Figure 15. Table showing analysis method.

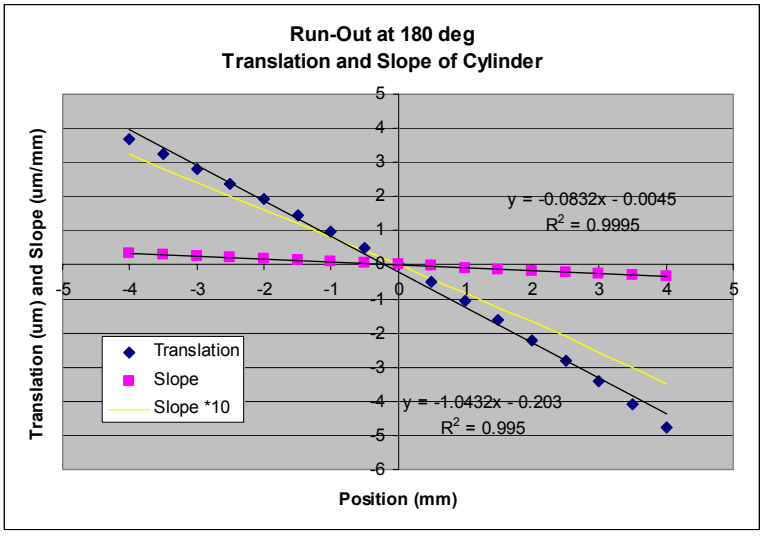

Figure 16. Case 3: Slope and Translation of Cylinder.

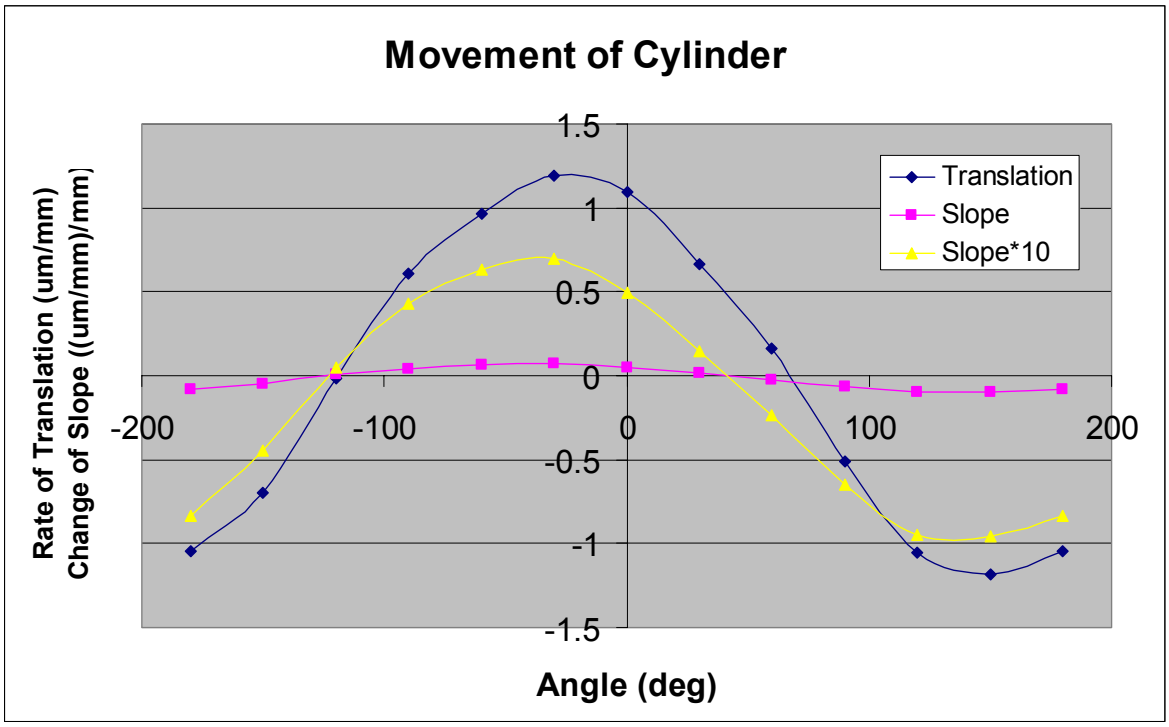

Figure 17. Movement of Cylinder. As expected, readings 180° apart are equal and opposite.

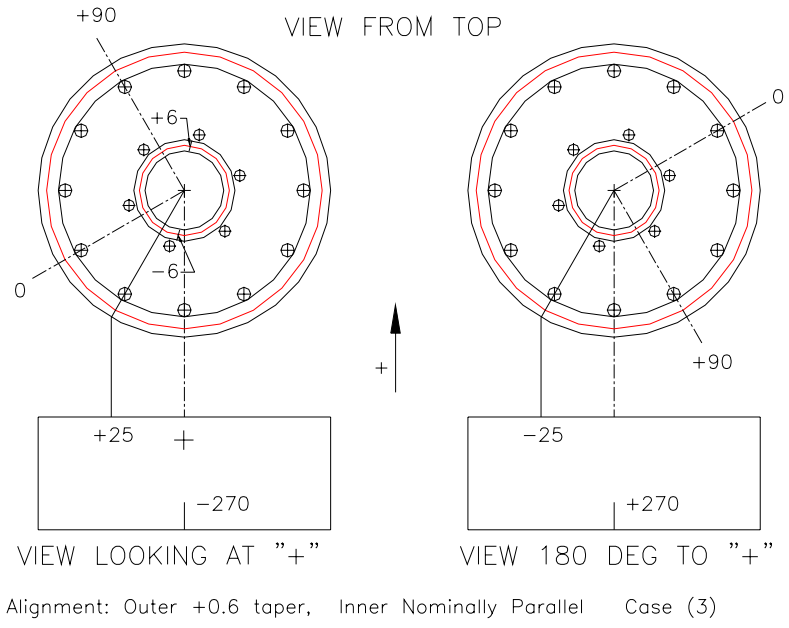

Figure 18. Alignment of Case (3). Taking the datum as the bore of the Inner Cylinder, the Outer Cylinder has a low run-out at the top (varying from +25 to -25 microns), and high run-out at the bottom (+270 to -270). Hence there is angular misalignment between the Inner and the Outer Cylinders.

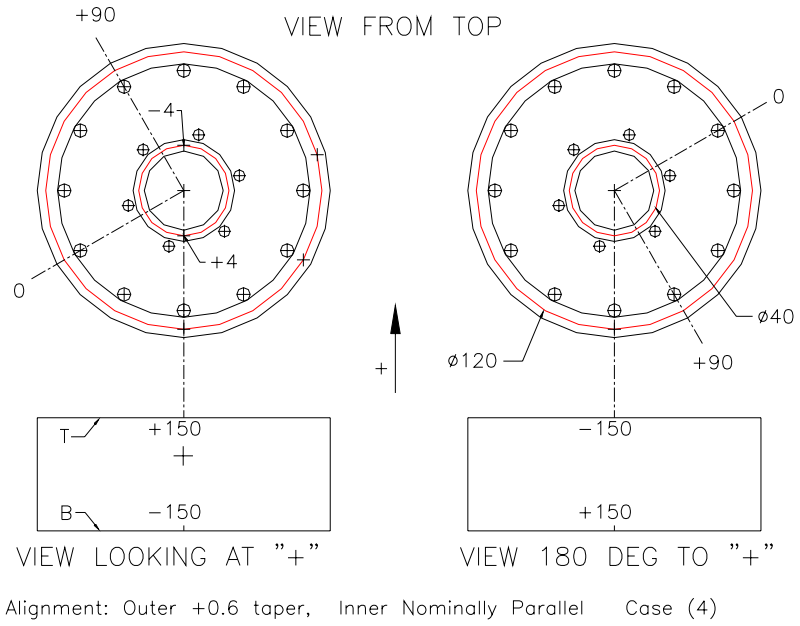

Figure 19. Alignment of Case (4). Taking the datum as the bore of the Inner cylinder, the run-out of the Outer cylinder is symmetrically disposed between top and bottom, hence there is minimal angular misalignment between the Inner and Outer Cylinders.

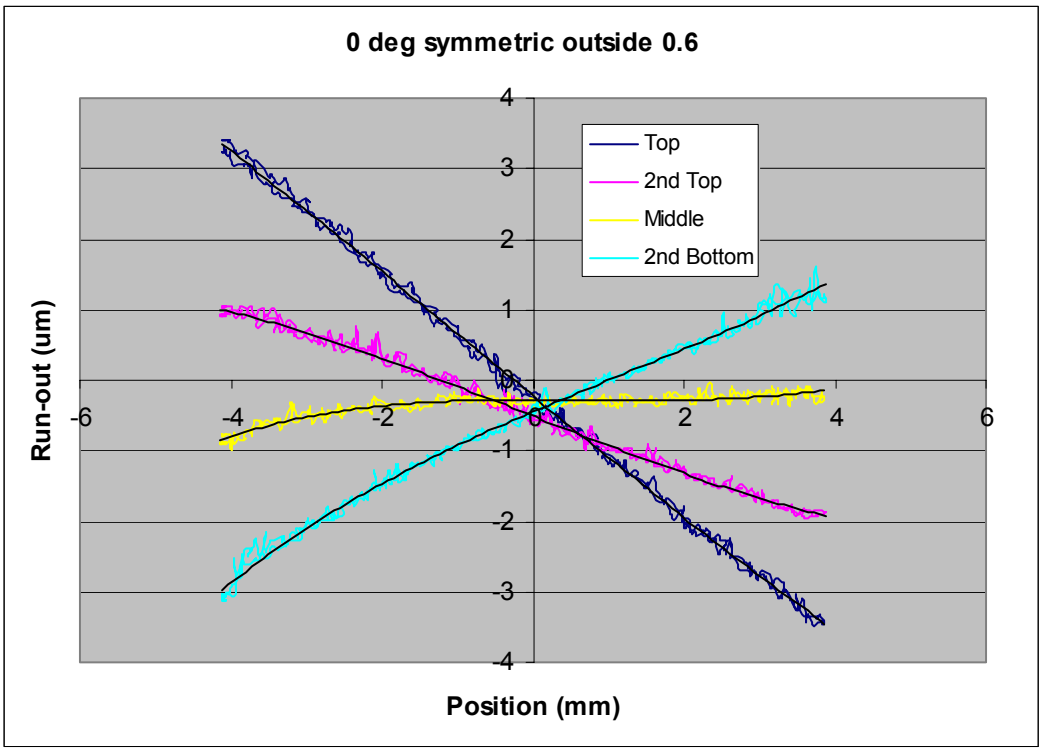

Figure 20. Case 4: Run-out measurements. Inner Parallel, Outer 0.6 Tapered and Aligned.

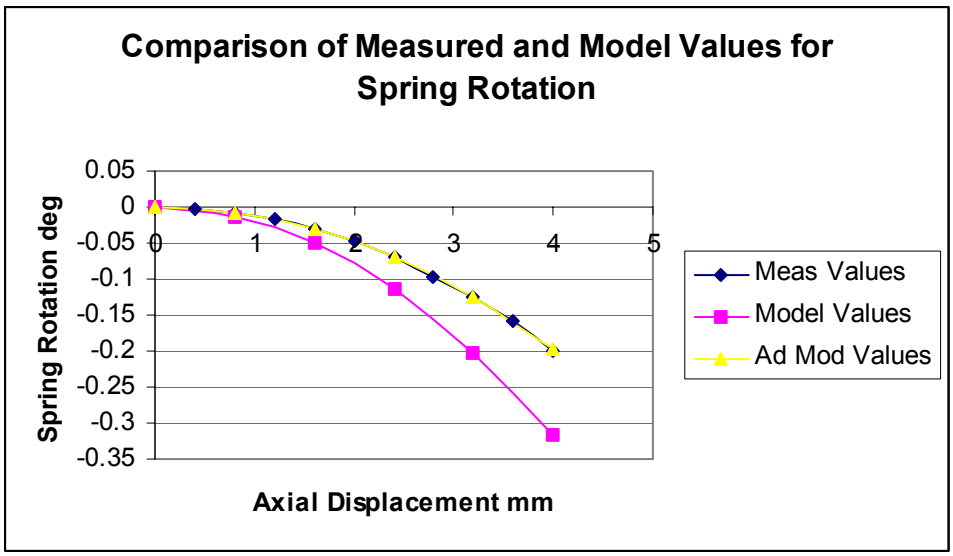

Figure 21. Measured and Model Values for Spring Rotation.

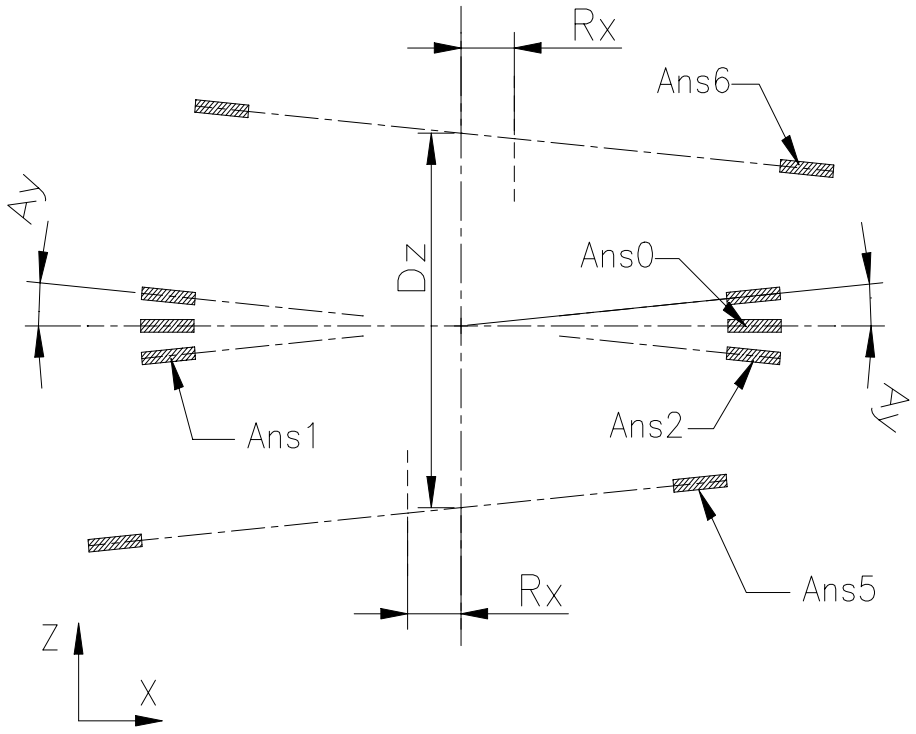

Figure 22. Geometry of Mis-aligned Surfaces.

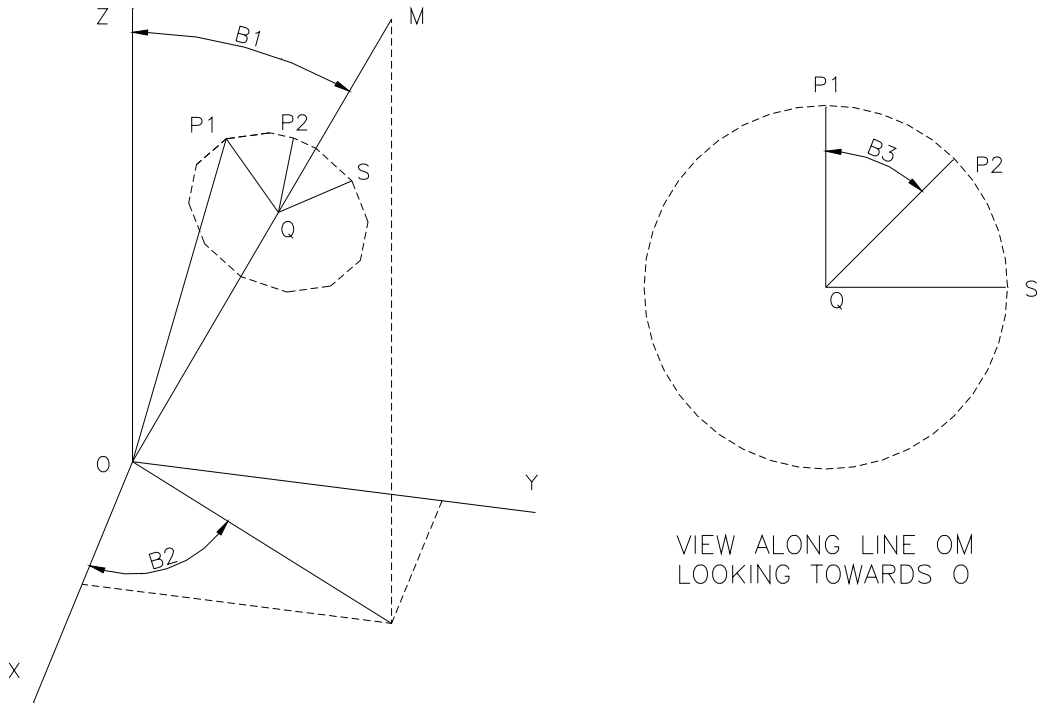

Figure 23. Definition of Axes and Angles.

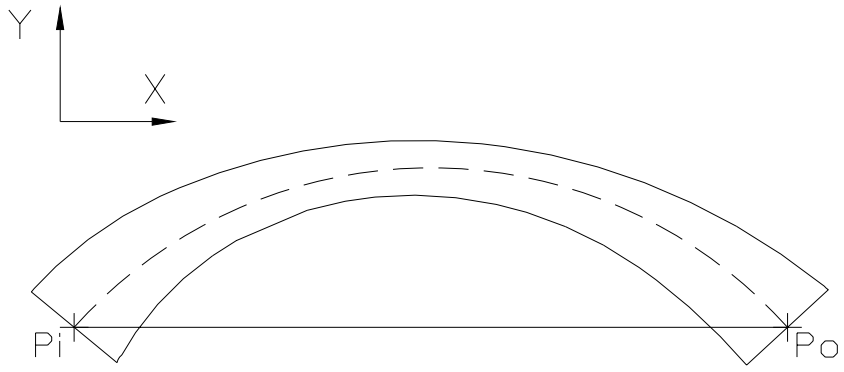

Figure 24. Geometry of A Single Spiral Spring Arm.

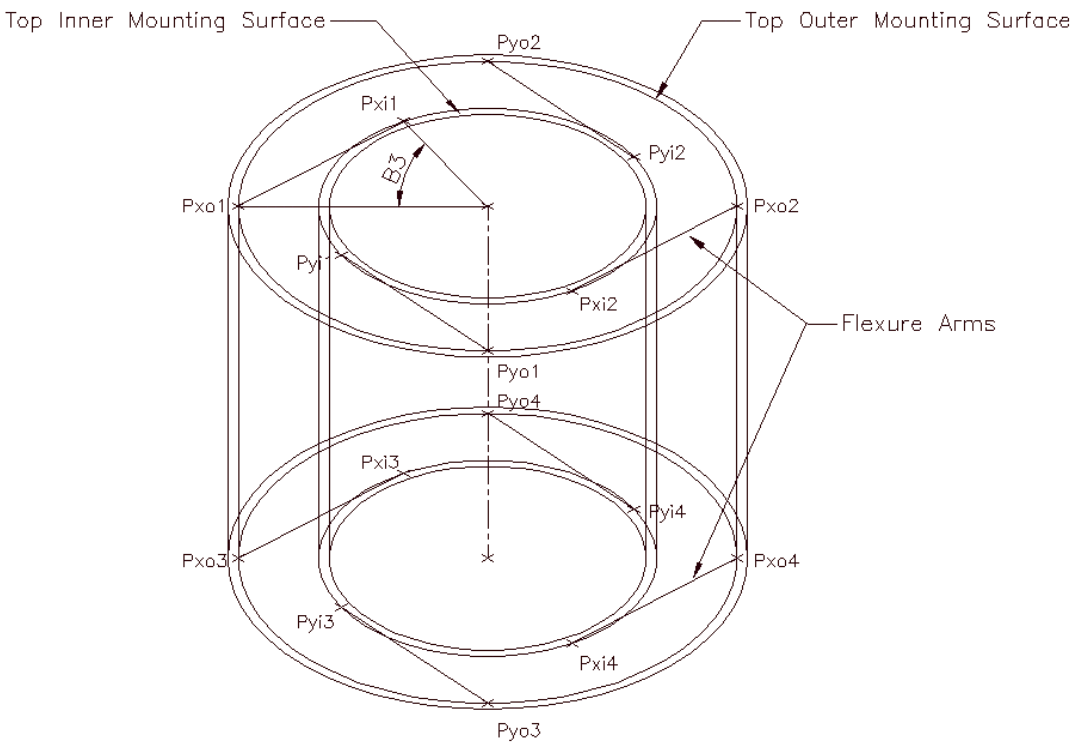

Figure 25. Flexure Spring Model

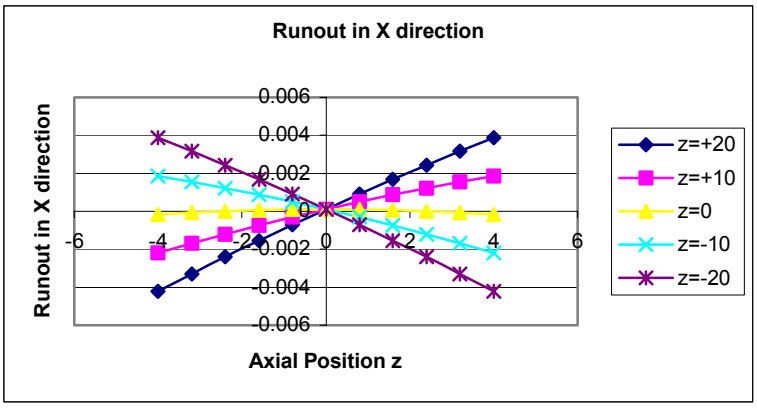

Figure 26. Runout in X direction for case #5

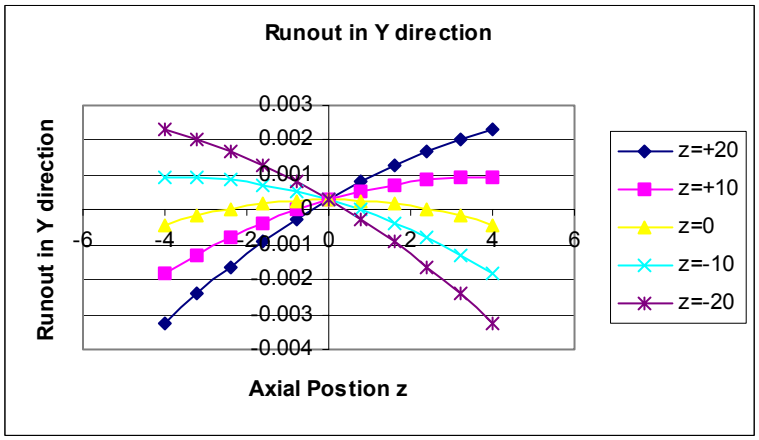

Figure 27. Runout in Y direction for case #5.

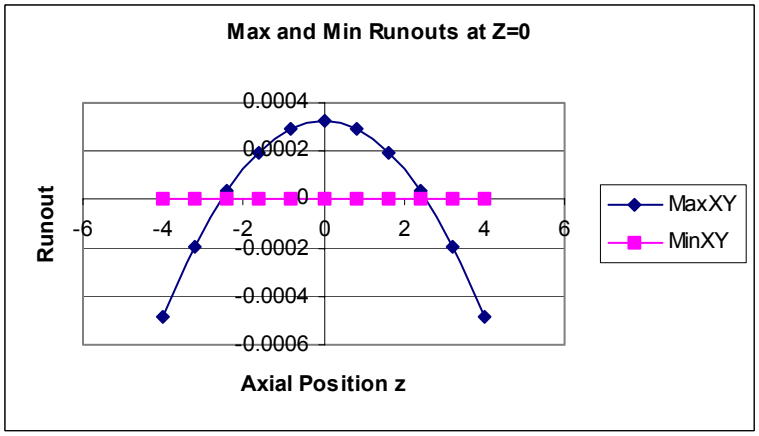

Figure 28. Maximum and Minimum Runouts at Z =0 for case #5

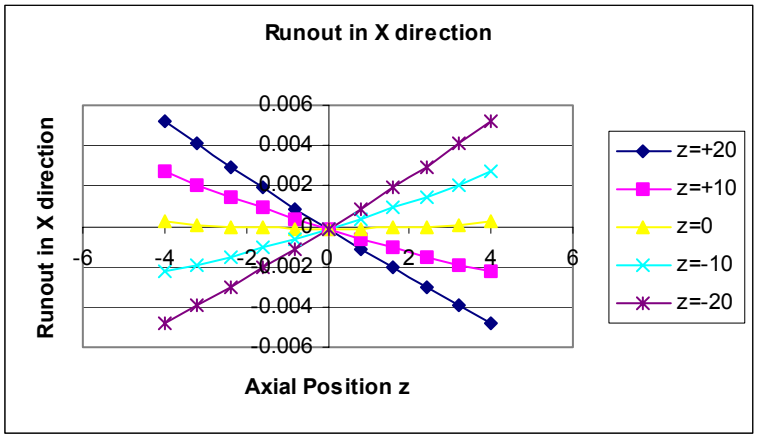

Figure 29. Runout in X direction for case #6

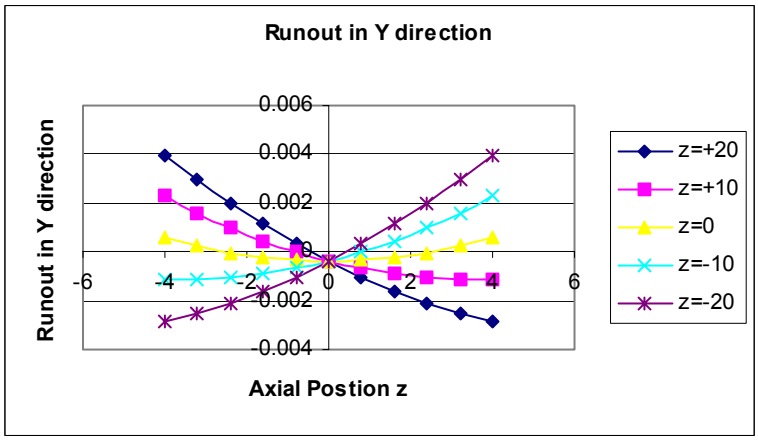

Figure 30. Runout in Y direction for case #6

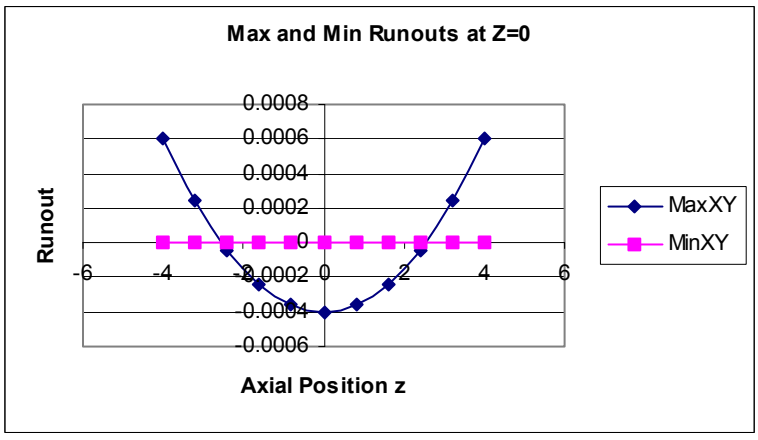

Figure 31. Maximum and Minimum Runouts at Z =0 for case #6

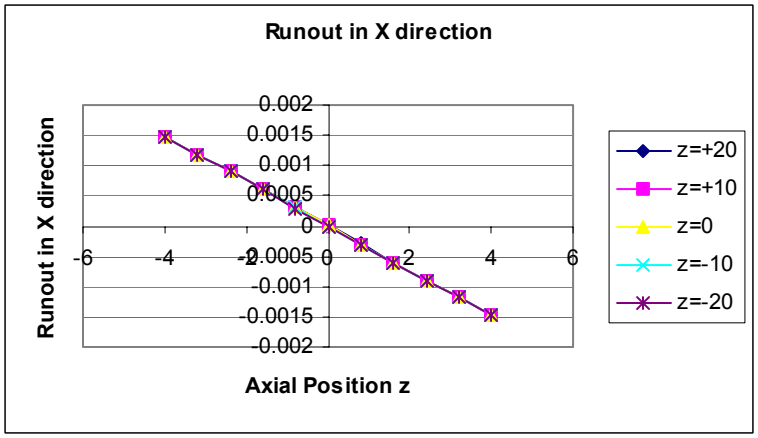

Figure 32. Runout in X direction for case #7

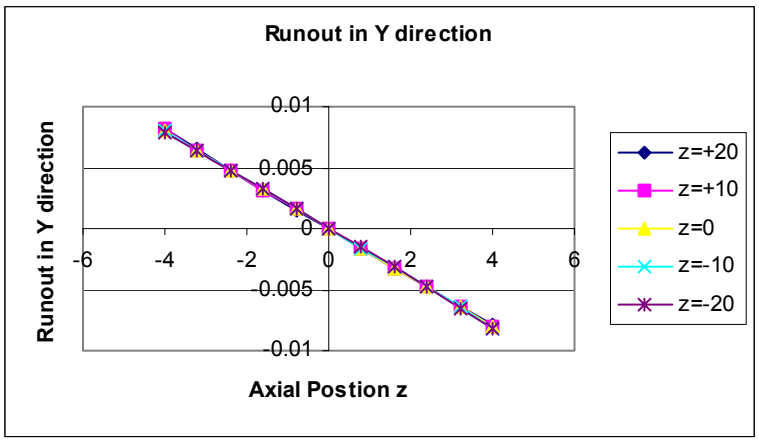

Figure 33. Runout in Y direction for case #7

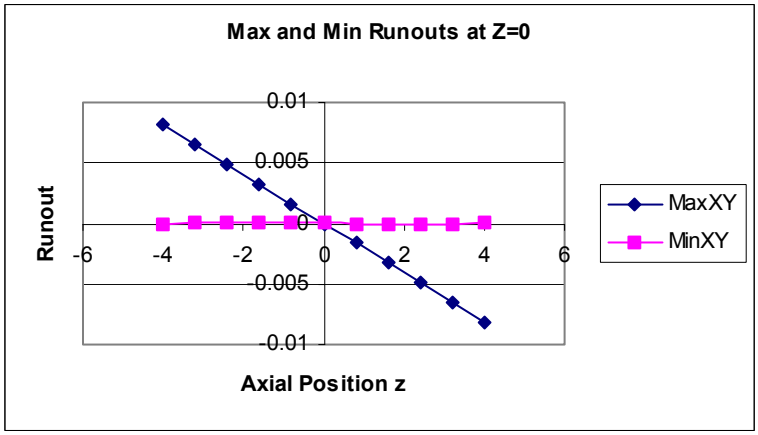

Figure 34. Maximum and Minimum Runouts at Z =0 for case #7

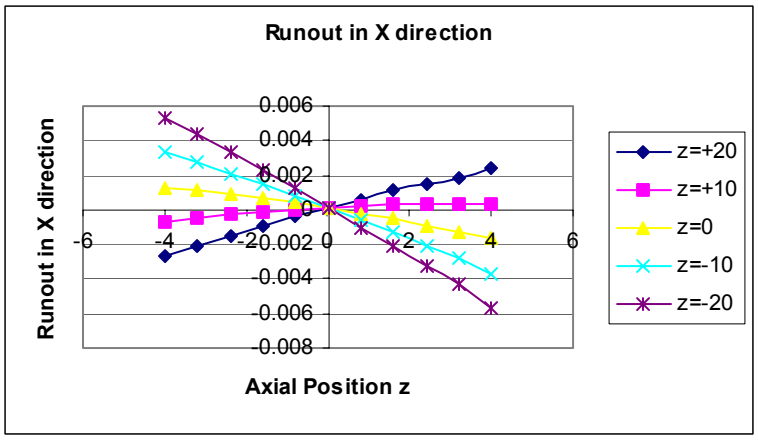

Figure 35. Runout in X direction for case #8

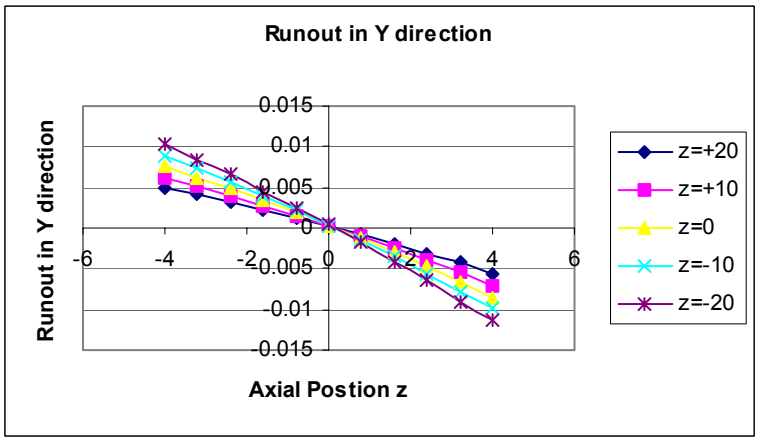

Figure 36. Runout in Y direction for case #8

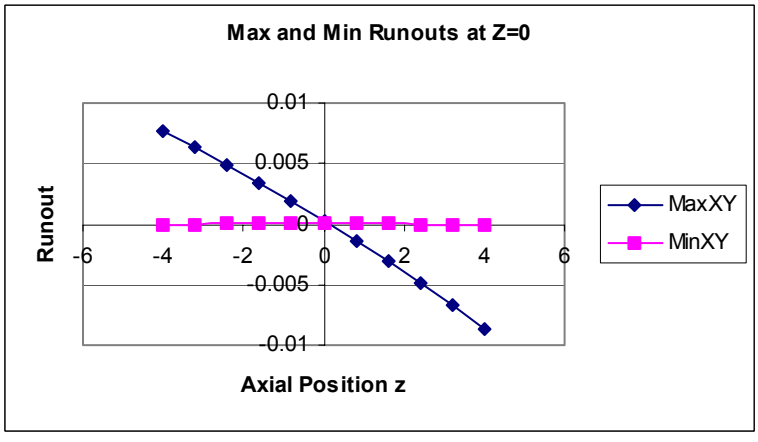

Figure 37. Maximum and Minimum Runouts at Z =0 for case #8

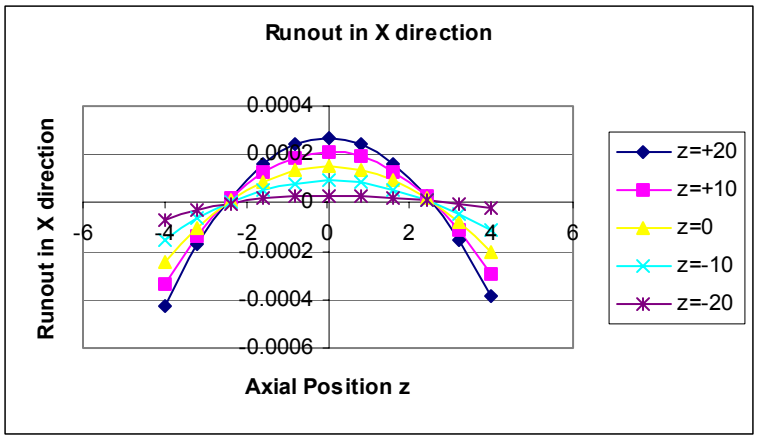

Figure 38. Runout in X direction for case #9

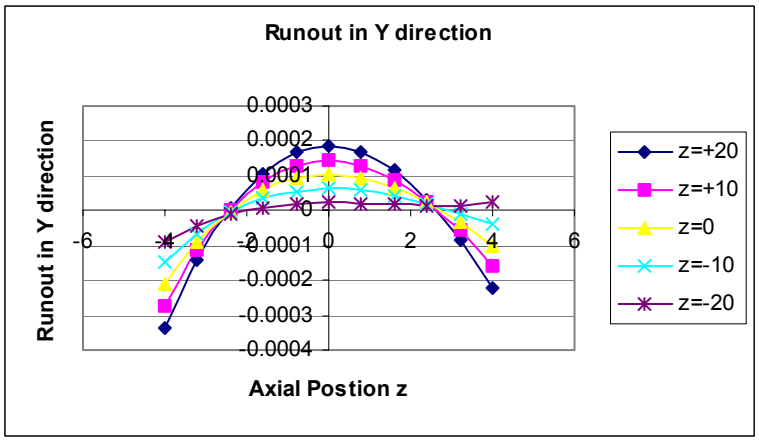

Figure 39. Runout in Y direction for case #9

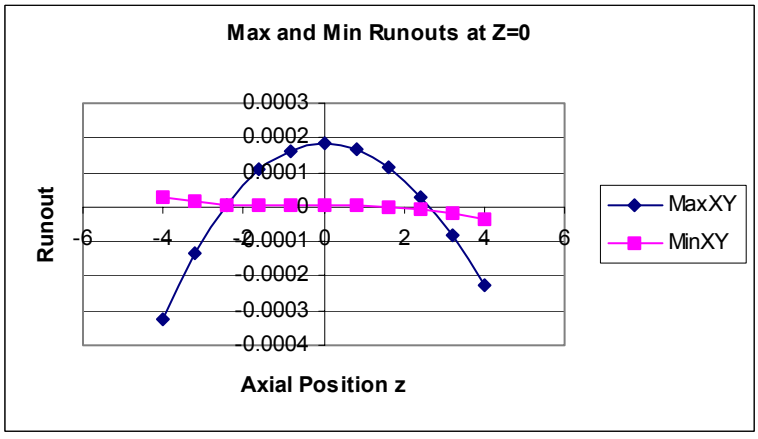

Figure 40. Maximum and Minimum Runouts at Z =0 for case #9